

However, including the $1+0.2/W$ term in the shape factor of the outer group gives an end-point energy of 0.780 ± 0.006 MeV for the inner group. This yields a value of 877 keV for the excited level of Kr⁸⁴, which is in much closer agreement.

Whether the correction factor is applied to the outer group or not, however, the shape of the inner group deviates from that of an allowed spectrum. This deviation cannot be accounted for by an empirical correction factor of the form $1+0.3/W$ alone. Such a factor has been found compatible with the shapes of other well-

measured spectra. Hence, it is reasonable to expect that it should apply in this case also. Thus, the inner β^+ transition does appear to have a shape which is slightly, but measurably, different from the statistical shape. Although this small deviation from the statistical shape may not be sufficient to permit an explanation in terms of the modified B_{ij} approximation, it should be taken into account in any attempt at a detailed analysis involving all of the matrix elements.¹⁸

¹⁸ Such an explanation is being attempted by S. Wahlborn (private communication).

Photoneutron Cross Sections for Natural Cu, Cu⁶³, and Cu⁶⁵†

S. C. FULTZ, R. L. BRAMBLETT, J. T. CALDWELL, AND R. R. HARVEY

Lawrence Radiation Laboratory, University of California, Livermore, California

(Received 25 October 1963)

Using monochromatic gamma rays obtained from the annihilation-in-flight of fast positrons, the (γ, n) and $(\gamma, 2n)$ cross sections for samples of natural Cu, Cu⁶³ enriched to 99.3% and Cu⁶⁵ enriched to 99.7% were measured. The (γ, n) cross sections for natural Cu, Cu⁶³, and Cu⁶⁵ were found to have maximum values of 71 ± 7 , 70 ± 7 , and 75 ± 7 mb, respectively, while the maximum $(\gamma, 2n)$ cross sections are 15.4 ± 2 , 13.5 ± 1 , and 28 ± 3 mb, respectively. The corresponding values for the (γ, n) integrated cross sections up to 28 MeV are 525 ± 52 , 523 ± 52 , and 437 ± 43 MeV-mb, and the $(\gamma, 2n)$ integrated cross sections are 110 ± 11 , 80 ± 8 , and 195 ± 19 MeV-mb.

THE (γ, n) cross section of copper has been used extensively as a standard for the measurement of photonuclear cross sections. The 9.8-min half-life of Cu⁶², resulting from Cu⁶³(γ, n) reaction, is convenient for measurement. The activity of the 12.8-h Cu⁶⁴ can also be easily measured. Thus, the copper (γ, n) cross section may be measured either by activation or neutron detection, and the results of many experiments have been presented relative to it. The activation technique has the advantage that the cross section for a single isotope is determined. To achieve this advantage in experiments which detect neutrons, separated isotopes must be used.

Previous measurements on (γ, n) and (γ, p) reactions in copper have been performed using photons from charged-particle reactions and electron bremsstrahlung. For those measurements using bremsstrahlung, either activation curves or neutron-yield curves were obtained and these were unfolded by standard techniques in order to obtain the cross sections. In the work described herein, cross sections for (γ, n) and $(\gamma, 2n)$ reactions in natural Cu, Cu⁶³, and Cu⁶⁵ were measured by use of nearly monoenergetic photons obtained from the annihilation-in-flight of fast positrons. The $(\gamma, 2n)$ cross section was determined by counting those cases in which

one, two, or three neutrons were detected following a pulse of photons.

EXPERIMENTAL METHOD

Positrons were created in a thick tungsten target located at the end of the first section of a two-section linear electron accelerator. They were then accelerated to the desired energy by adjusting the rf power and phase in the second section. The positrons were energy analyzed by a magnet and a two-jaw slit. The nearly monochromatic positrons then passed through a thin LiH target in which some annihilated in flight by two-photon annihilation. In this process, the photon moving in the forward direction has about 0.76 MeV more energy than the positron. Multiple scattering in the LiH target caused a photon energy spread of approximately 3%. Those positrons which penetrated the target were swept away by a strong magnet. The photon flux was measured by use of a transmission ion chamber filled with xenon to a pressure of 1 atm. This chamber was calibrated with a gamma-ray spectrometer having a 6-in.-long \times 5-in.-diam NaI(Tl) crystal.

The photons were incident (in 2- μ sec pulses) on copper samples placed in a 4π neutron detector having an efficiency of about 20%. This paraffin-moderated neutron detector contained 24 BF₃ proportional counters filled to 120 cm Hg with 96% enriched B¹⁰. The gating

† Work done under the auspices of the U. S. Atomic Energy Commission.

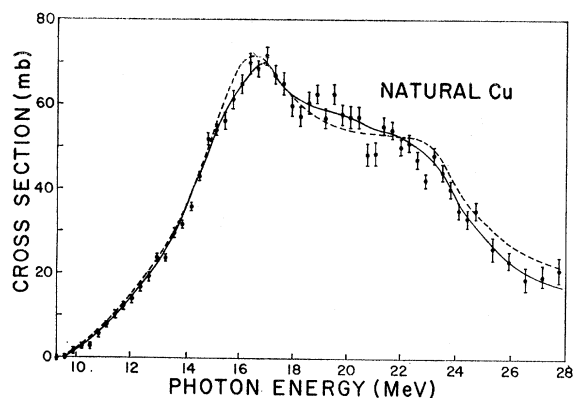


FIG. 1. Solid curve gives the average of data points of the total cross section $[\sigma(\gamma, n) + 2\sigma(\gamma, 2n) + \sigma(\gamma, np)]$ for natural Cu. The dashed line represents the total cross section given by the sum of the total cross sections measured for Cu^{63} and Cu^{65} and adjusted for isotopic abundances.

interval for the neutron counts was 335 μsec and the counts were separated electronically as single, double, or triple counts during the gating interval, each gating interval corresponding to one beam pulse. The neutron counts recorded per beam pulse were correlated to the number of neutrons emitted per nuclear disintegration by statistical analysis and the cross sections for the (γ, n) and $(\gamma, 2n)$ reactions could then be deduced. More details of the experimental procedure are given in previous reports.¹⁻³

A. Natural Cu (γ, n) and $(\gamma, 2n)$ Cross Sections

There exist several bremsstrahlung measurements on natural copper. Byerly and Stephens⁴ examined the ratio of neutrons, deuterons, and alpha particles to protons for natural copper. They used the nuclear emulsion technique with bremsstrahlung irradiations and obtained 2.8, 0.31, and 0.03 for ratios n/p , d/p , and α/p , respectively. Montalbetti, Katz, and Goldemberg⁵ obtained a peak (γ, n) yield of 120 mb at 19.5 MeV. They also obtained an integrated yield, $\sigma(\gamma, n) + 2\sigma(\gamma, 2n) + \sigma(\gamma, np)$, of 0.87 MeV-b, and an integrated cross section for $\sigma(\gamma, 2n)$ of 0.054 MeV-b for the energy range up to 23 MeV. Jones and Terwilliger⁶ obtained the expression $5.2 \times 10^{-4} A^{1.8}$ MeV-b for the integrated cross section up to 27.5 MeV. This would give 0.904 MeV-b for natural Cu. Miller, Schuhl, and Tzara,⁷ using nearly monochromatic photons obtained from the annihilation-

in-flight of positrons, obtained a peak cross section of approximately 90 mb at 16.9 MeV and an integrated total cross section of 0.45 ± 0.015 MeV-b for photon energies up to 19.6 MeV. Gavrilov and Lazareva⁸ obtained a peak cross section of 126 mb at 17.2 MeV and an integrated cross section of 0.93 MeV-b.

For the present experiment, the sample consisted of 115 g of natural Cu, which contains 60.09% Cu^{63} and 30.91% Cu^{65} . It was constructed of a disk, 2 in. in diameter by 0.25 in. thick, mounted in a plastic foam container and placed at the center of the paraffin-moderated detector. Results obtained from the experiment are shown in Figs. 1 and 2. In Fig. 1 is shown the neutron yield curve, $\sigma(\gamma, n) + 2\sigma(\gamma, 2n) + \sigma(\gamma, np)$. Figure 2 shows the (γ, n) and $(\gamma, 2n)$ cross section curves for natural copper. As can be seen in Figs. 1 and 2, the neutron yield and the (γ, n) cross section curves have a peak value of 71 ± 7 mb at approximately 16.75 MeV. The $(\gamma, 2n)$ cross-section curve has a broad maximum of 15.4 ± 2 mb at approximately 23 MeV. The thresholds observed for the (γ, n) and $(\gamma, 2n)$ reactions at 9.75 ± 0.2 and 18.0 ± 0.3 MeV are due to the thresholds of Cu^{65} .

A number of cross-section measurements on natural Cu have been made by use of the monochromatic gamma rays obtained from the $\text{Li}^7(p, \gamma)\text{Be}^8$ reaction. McDaniel, Walker, and Stearns⁹ obtained a cross section of 55 ± 12 mb; Hartley, Stephens, and Winhold¹⁰ obtained 64 ± 10 mb, while Carver and Kondaiah¹¹ obtained 85 ± 15 mb. Assuming that the ratio of the intensities of the 17.6- to 14.8-MeV gamma rays is 2.1,¹² the total photoneutron

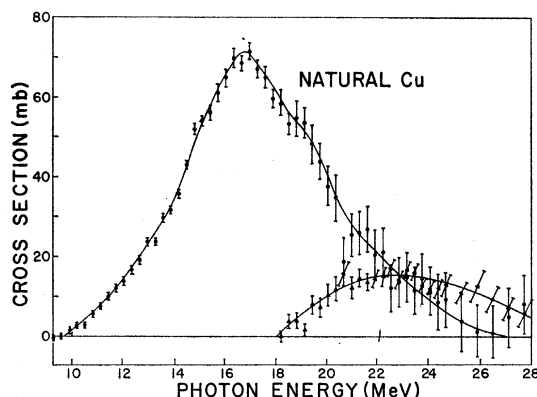


FIG. 2. Measured cross sections for (γ, n) and $(\gamma, 2n)$ reactions on natural Cu. The top curve was obtained from single-neutron counting data and consists of $\sigma(\gamma, n) + \sigma(\gamma, np)$. The lower curve consists of $\sigma(\gamma, 2n)$ and was obtained from double-neutron counting data.

¹ S. C. Fultz, R. L. Bramblett, J. T. Caldwell, and N. A. Kerr, *Phys. Rev.* **127**, 1273 (1962).

² S. C. Fultz, R. L. Bramblett, J. T. Caldwell, N. E. Hansen, and C. P. Jupiter, *Phys. Rev.* **128**, 2345 (1962).

³ R. L. Bramblett, J. T. Caldwell, G. F. Auchampaugh, and S. C. Fultz, *Phys. Rev.* **129**, 2723 (1963).

⁴ P. R. Byerly, Jr. and W. E. Stephens, *Phys. Rev.* **81**, 473 (1951).

⁵ R. Montalbetti, L. Katz, and J. Goldemberg, *Phys. Rev.* **91**, 659 (1953).

⁶ L. W. Jones and K. M. Terwilliger, *Phys. Rev.* **91**, 699 (1953).

⁷ J. Miller, C. Schuhl, and C. Tzara, *Nucl. Phys.* **32**, 236 (1962).

⁸ B. I. Gavrilov and L. E. Lazareva, *Zh. Eksperim. i Teor. Fiz.* **30**, 855 (1956) [English transl.: *Soviet Phys.—JETP* **3**, 871 (1957)].

⁹ B. D. McDaniel, R. L. Walker, and M. B. Stearns, *Phys. Rev.* **80**, 807 (1950).

¹⁰ W. H. Hartley, W. E. Stephens, and E. J. Winhold, *Phys. Rev.* **104**, 178 (1956).

¹¹ J. H. Carver and E. Kondaiah, *Phil. Mag.* **45**, 988 (1954).

¹² V. Meyer, H. Muller, H. H. Staub, and R. Zurmuhle, *Nucl. Phys.* **27**, 284 (1961).

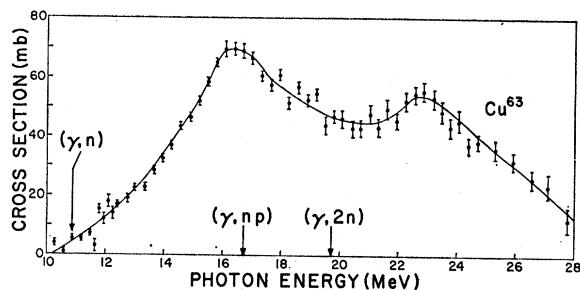


Fig. 3. Total cross section $[\sigma(\gamma, n) + 2\sigma(\gamma, 2n) + \sigma(\gamma, np)]$ for Cu^{63} obtained from single-neutron counting data.

cross section corresponding to the Li gamma rays as deduced from the results of the present experiment, is 61 ± 6 mb, in good agreement with McDaniel *et al.* and Hartley *et al.*

B. $\text{Cu}^{63}(\gamma, n)$ and $(\gamma, 2n)$ Cross Sections

The $\text{Cu}^{63}(\gamma, n)\text{Cu}^{62}$ cross section has been measured previously by bremsstrahlung activation of 9.8-min Cu^{62} . Johns *et al.*¹³ obtained 0.070 MeV-b for the integrated cross section up to 25 MeV. Strauch,¹⁴ using 300-MeV bremsstrahlung, obtained an integrated cross section of 0.76 MeV-b. Katz *et al.*^{5,15} obtained a peak in the total cross section curve of 104 mb at 18 MeV, and an integrated cross section of 0.66 MeV-b up to 25 MeV. Krohn and Shrader¹⁶ obtained a peak cross section of 94 mb at 17.0 MeV when using D_2O -loaded emulsions and a pair spectrometer to monitor the photons. Berman and Brown¹⁷ measured (γ, n) and $(\gamma, 2n)$ cross sections by the activation method. They obtained 0.55 ± 0.03 and 0.081 MeV-b for the integrated cross sections of the (γ, n) and $(\gamma, 2n)$ reactions respectively, up to an energy of 35 MeV. The corresponding peak cross sections for these reactions were approximately 98 and 12 mb at 17 and 25.5 MeV, respectively.

The Cu^{63} sample used in the present experiment consisted of 2-in.-diam disks of metallic Cu enriched to 99.35% Cu^{63} , weighing a total of 50 g. Results from the experiment are shown in Figs. 3, 4, and 5 and Table I. In Fig. 3 is shown the total cross-section curve, $\sigma(\gamma, n) + 2\sigma(\gamma, 2n) + \sigma(\gamma, np)$. The (γ, n) and $(\gamma, 2n)$ cross sections are shown in Fig. 4, while the sum $\sigma(\gamma, n) + \sigma(\gamma, np) + \sigma(\gamma, 2n)$ is shown in Fig. 5. The width at half-maximum Γ for the compound nucleus formation cross section (Fig. 5) is 8.5 MeV, and is considerably broader than any previously reported; see Refs. 4, 5, 8, 16, and 17, where Γ has values ranging from 4.9 and 7.1 MeV.

The integrated cross sections given in Table I represent values which have been measured and calculated. The contribution of the (γ, np) and (γ, p) reactions were

TABLE I. Integrated cross sections up to 28 MeV for copper isotopes.

Element	Reaction	Integrated cross section (MeV-mb)	Fraction of total integrated cross section	Total (MeV-mb)
Natural Cu	$(\gamma, n) + (\gamma, np)$	525 ± 52	0.67	787 ± 113
	$(\gamma, 2n)$	110 ± 11	0.14	
	$(\gamma, p)^a$	152 ± 50	0.19	
Cu^{63}	$(\gamma, n) + (\gamma, np)$	523 ± 52	0.89	764 ± 09
	+direct			
	$(\gamma, 2n)$	80 ± 8	0.11	
	$(\gamma, np)^a$	115 ± 20	0.15	
	$(\gamma, p)^a$	161 ± 48	0.21	
	(γ, n)	344 ± 34	0.45	
Cu^{65}	$(\gamma, n) + (\gamma, np)$	437 ± 43	0.57	766 ± 103
	$(\gamma, 2n)$	195 ± 19	0.25	
	$(\gamma, p)^a$	134 ± 40	0.18	

^a Calculated from evaporation theory.

^b Estimated.

^c See Ref. 20.

calculated by use of the evaporation model. The "direct" interaction estimate was deduced by calculating $\sigma(\gamma, n)$ and $\sigma(\gamma, np)$ from the measured $\sigma(\gamma, 2n)$ in the high-energy region, and subtracting the calculated sum $\sigma(\gamma, n) + \sigma(\gamma, np)$ from the measured single-neutron cross-section curve. Thus, the "direct" component represents that portion of the cross-section curve which cannot be accounted for on the basis of evaporative processes. The thresholds for the (γ, n) and $(\gamma, 2n)$ reactions were found to be 10.4 ± 0.3 and 19.0 ± 0.8 MeV.

The Li gamma rays have been used extensively to measure the $\text{Cu}^{63}(\gamma, n)\text{Cu}^{62}$ reaction cross section. An excellent summary of this work is given by Coote *et al.*¹⁸ A summary of some of the results formerly obtained is given in Table II. The average value for the neutron yield is 64 ± 4 mb. Omitting that obtained from Ref. a,

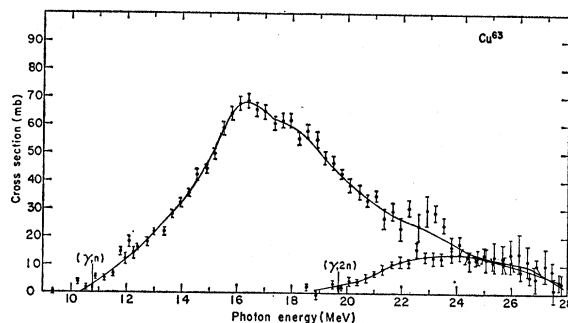


Fig. 4. Partial cross sections measured for Cu^{63} . The top curve consists of $\sigma(\gamma, n) + \sigma(\gamma, np)$ plus contributions from direct interactions and was obtained from single-neutron counting data. The lower curve consists of $\sigma(\gamma, 2n)$ and was obtained from double-neutron counting data.

¹³ H. E. Johns, L. Katz, L. Douglas, and R. N. H. Haslam, Phys. Rev. 80, 1062 (1950).

¹⁴ K. Strauch, Phys. Rev. 81, 973 (1951).

¹⁵ L. Katz and A. G. W. Cameron, Can. J. Phys. 29, 518 (1951).

¹⁶ V. E. Krohn and E. F. Shrader, Phys. Rev. 87, 685 (1952).

¹⁷ A. I. Berman and K. L. Brown, Phys. Rev. 96, 83 (1954).

¹⁸ G. E. Coote, W. E. Turchinets, and I. F. Wright, Nucl. Phys. 23, 468 (1961).

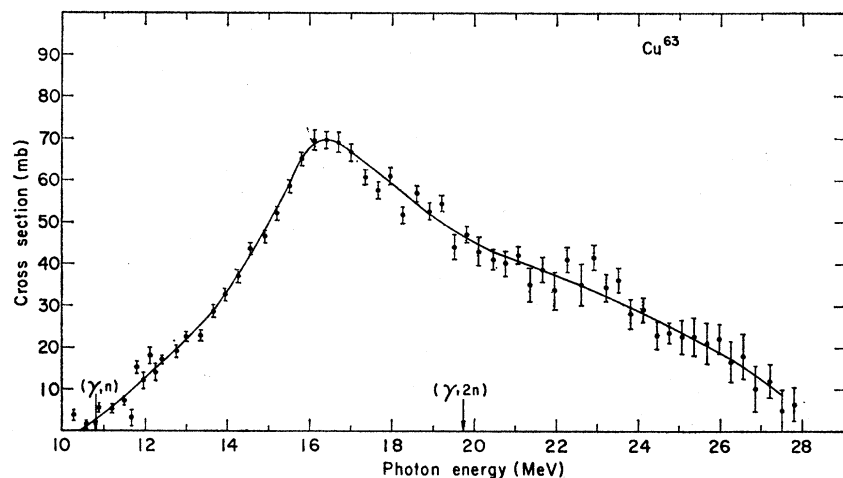


FIG. 5. The formation cross section of Cu^{65} , $\sigma(\gamma,n) + \sigma(\gamma,np) + \sigma(\gamma,2n) + \sigma_{\text{direct}}$. Contributions from $\sigma(\gamma,p)$ are not included here.

Table II, which appears to be considerably higher than the others, the mean value becomes 57 ± 3 mb. The latter is in good agreement with 55 ± 6 mb obtained in the present experiment. Del Bianco and Stephens,¹⁹ using monochromatic photons obtained from the $\text{T}^3(p,\gamma)\text{He}^4$ reaction, obtained a value of 52.5 ± 2.5 mb at 20.5 MeV, which is somewhat higher than 36 ± 4 mb obtained in the present experiment.

TABLE II. Cross section for Li gamma rays.

Natural Cu	Cu^{68}	Cu^{65}	Reference
$\sigma(\gamma,n)$ (mb)	$\sigma(\gamma,n)$ (mb)	$\sigma(\gamma,n)$ (mb)	
55 ± 12	120 ± 30		a
	52 ± 11		b
	48 ± 8		c
85 ± 15	80 ± 14		d
64 ± 10	60 ± 9		e
	38 ± 6		f
	64 ± 4		g
	59 ± 6	70 ± 7	h
61 ± 6	55 ± 6	66 ± 6	Present work ⁱ

- a H. Waffler and O. Hirzel, *Helv. Phys. Acta* **25**, 491 (1952).
 b See Ref. 9.
 c H. Glätti, O. Seippel, and P. Stoll, *Helv. Phys. Acta* **25**, 491 (1952).
 d See Ref. 11.
 e See Ref. 10.
 f T. Nakamura, K. Takamatsu, K. Fukunaga, M. Yata, and S. Yasumi, *J. Phys. Soc. Japan* **14**, 693 (1959).
 g S. Yasumi, M. Yata, K. Takamatsu, A. Masaike, and Y. Masuda, *J. Phys. Soc. Japan* **15**, 1913 (1960).
 h See Ref. 18.
 i Calculated assuming that the ratio of intensities for the 17.6- to 14.8-MeV Li gamma rays is 2.1.

C. $\text{Cu}^{65}(\gamma,n)$ and $(\gamma,2n)$ Cross Sections

The (γ,n) cross section for Cu^{65} has been studied by use of bremsstrahlung through activation of Cu^{64} , which has a 12.8-h half-life for positron and negative beta-ray emission. Strauch¹⁴ obtained an integrated cross section of 0.99 MeV-b. Katz *et al.*^{5,15} found a peak cross section of 150 mb at 18.6 MeV and a (γ,n) in-

tegrated cross section of 1.11 MeV-b. The width at half-maximum for the integrated cross section is given as 7.0 MeV. Lin Kova *et al.*²⁰ examined the energy and angular distributions of protons produced in a Cu^{65} -enriched sample, using bremsstrahlung radiation and photographic emulsions. They concluded that at least 80% of the photoproton yield arises through direct interactions and that the sum of the integrated cross sections, $\sigma(\gamma,p) + \sigma(\gamma,np)$, is approximately 20% of the total. They obtained 0.190 MeV-b for the $\sigma(\gamma,p) + \sigma(\gamma,np)$ integrated cross section up to 25 MeV.

The Cu^{65} sample consisted of 50 g of Cu^{65} enriched to 99.7%. Results from the measurements are shown in Figs. 6, 7, and 8 and in Table I. In Fig. 6 is shown the yield curve for Cu^{65} . The (γ,n) and $(\gamma,2n)$ cross-section curves are given in Fig. 7, while the compound nucleus formation cross section is given in Fig. 8. In Fig. 8 the data points give the sum of the $\sigma(\gamma,n)$ and $\sigma(\gamma,2n)$ measurements. The dashed line gives the nuclear-formation cross section which was deduced by adding to this sum the $\sigma(\gamma,p)$ cross-section curve given by Lin Kova *et al.*²⁰

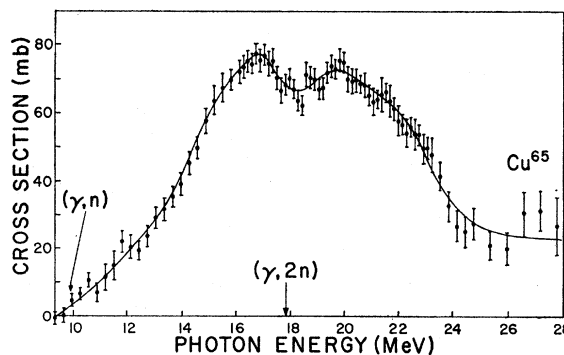


FIG. 6. Total cross section [$\sigma(\gamma,n) + 2\sigma(\gamma,2n) + \sigma(\gamma,np)$] for Cu^{65} obtained from single-neutron counting data.

²⁰ N. V. Lin Kova, R. M. Osokina, B. S. Ratner, R. Sh. Amirov, and V. V. Akindinov, *Zh. Eksperim. i Teor. Fiz.* **38**, 780 (1960) [English transl.: *Soviet Phys.—JETP* **11**, 566 (1960)].

¹⁹ W. E. Del Bianco and W. E. Stephens, *Phys. Rev.* **126**, 709 (1962).

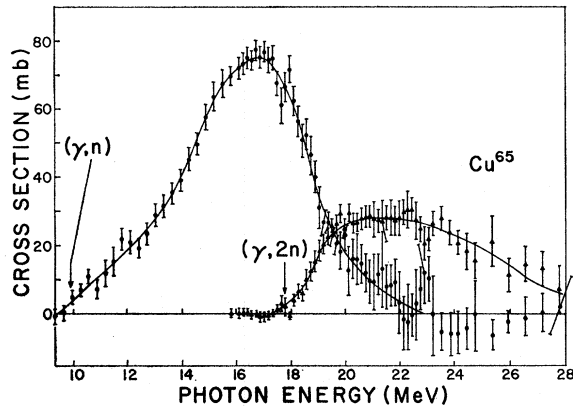


FIG. 7. Partial cross sections for Cu^{65} . The top curve consists of $\sigma(\gamma, n) + \sigma(\gamma, np)$. The lower curve consists of $\sigma(\gamma, 2n)$ and was obtained from double-neutron counting data.

For this work the ratio of yields of protons to neutrons was measured, and the (γ, p) cross section was obtained by normalizing to early (γ, n) cross-section measurements.¹⁵ The results were therefore renormalized to the present (γ, n) cross-section measurements. The peak cross section for the giant resonance of Cu^{65} is 87 ± 10 mb while the width Γ is 8.1 MeV.

The integrated cross sections up to 28 MeV for $\sigma(\gamma, n)$, $\sigma(\gamma, 2n)$, and $\sigma(\gamma, p)$ are shown in Table I. The contributions from (γ, np) reactions would be present in the $\sigma(\gamma, n)$ data and also the $\sigma(\gamma, p)$ data.²⁰ The (γ, np) threshold occurs at 17.1 MeV for Cu^{65} . If the cross sections for (γ, np) and "direct" reactions were appreciable, the high-energy portion of the single-neutron cross-section curve would exhibit a high-energy tail as was the case for Cu^{63} . However, as can be seen in Fig. 7, the single-neutron cross section becomes zero beyond 23 MeV. This is evidence that the contribution to the cross section from the (γ, np) and "direct" reactions is small. Thus, the fact that twice the (γ, np) cross section appears in the integrated cross sections presented in Table I does not cause serious error.

Results obtained for the Li gamma rays by Coote *et al.*¹⁸ are shown in Table II. The Li gamma ray cross section for Cu^{65} , 70 ± 7 mb, is in reasonable agreement with 66 ± 6 mb calculated from the data of the present experiment.

The self-consistency of the cross-section data taken on the copper isotopes and natural copper may be checked by comparing the yield curve for natural Cu with that deduced from the yield curves of Cu^{63} and Cu^{65} . This may be found by use of the expression

$$\sigma_{\text{nat}}(E) = 0.69\sigma_{63}(E) + 0.309\sigma_{65}(E),$$

where $\sigma_{\text{nat}}(E)$, $\sigma_{63}(E)$, and $\sigma_{65}(E)$ denote the yield cross sections at gamma-ray energy "E" for natural Cu, Cu^{63} , and Cu^{65} , respectively. The results of combining Figs. 3 and 6 in this manner are shown by the dashed line in Fig. 1. From this it can be seen that within the experimental errors the data appears to be self-consistent.

ANALYSIS

The calculated contribution from (γ, p) reactions to the integrated cross section of Cu^{63} is approximately 21%, while that for Cu^{65} is estimated to be 18% (Table I). Including these (γ, p) contributions, the integrated photon-absorption cross sections of Cu^{63} and Cu^{65} are 0.76 ± 0.11 and 0.77 ± 0.10 MeV-b, respectively, for photon energies up to 28 MeV. Lorentz curves were fitted to the data contained in Figs. 5 and 8. It was found that the data could be fitted equally well assuming either prolate or oblate spheroids for the shapes of the nuclei. Parameters for Lorentz curves deduced for these cases are given in Table III. Since the measured in-

TABLE III. Quadrupole moments and Lorentz line parameters.

Nuclear shape	Isotope	E_a (MeV)	σ_a (mb)	Γ_a (MeV)	E_b (MeV)	σ_b (mb)	Γ_b (MeV)	Q_0 (b)
Prolate Spheroid	Cu^{63}	16.00	48.5	3.5	19.0	44.5	7.5	1.1 ± 0.4
Prolate Spheroid	Cu^{65}	16.00	54.7	4.2	19.25	62.0	7.5	1.2 ± 0.4
Oblate Spheroid	Cu^{63}	16.50	62.5	5.0	21.25	22.0	7.1	-1.4 ± 0.4
Oblate Spheroid	Cu^{65}	16.75	87.5	5.0	20.5	36.4	6.0	-1.1 ± 0.4

tegrated cross section covers only the energy range up to 28 MeV, a correction must be made for contributions from 28 MeV to infinite energy in order that a meaningful comparison may be made with the theoretically derived integrated cross sections. This correction can be estimated from the shape of the Lorentz curve,² and is included in the third column of Table IV. The term "W" is the estimated correction to the integrated cross section. A comparison of the experimental data with the theoretical cross section derived through saturation of the dipole sum rule is obtained by comparing columns 3 and 4 of Table IV. It is evident that agreement is obtained within experimental error. Values deduced for the second moment of the cross section σ_{-2} are also given in Table IV. These may be compared with the theoretically derived quantities given in the last column of Table IV. It is evident that the measured and calculated

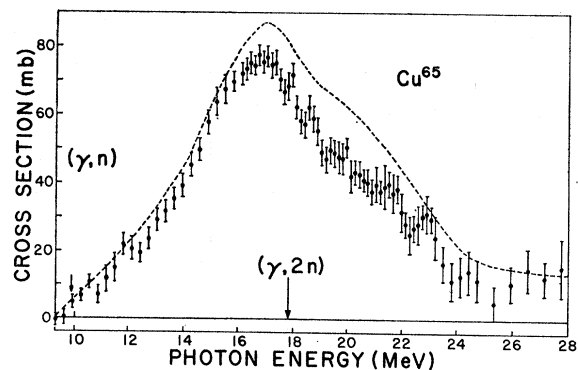


FIG. 8. The data points represent the sum $\sigma(\gamma, n) + \sigma(\gamma, np) + \sigma(\gamma, 2n)$. The dashed line represents the nuclear formation cross section $\sigma(\gamma, n) + \sigma(\gamma, 2n) + \sigma(\gamma, np) + \sigma(\gamma, p)$ for which the $\sigma(\gamma, p)$ data was obtained from Ref. 20.

TABLE IV. Integrated nuclear formation cross sections and σ_{-2} values.

Isotope	$\int_0^{28} \sigma dE$ (MeV-mb) ^a	$\int_0^{28} \sigma dE+W$ (MeV-mb) ^b	$0.06NZ/A$ (MeV-mb)	σ_{-2} (mb/MeV)	$0.00225 A^{5/3}$ (mb/MeV)
Cu ⁶³	764±109	913±121	939	2.1±0.3	2.4
Cu ⁶⁵	766±103	960±124	964	2.6±0.3	2.4

^a The integrated cross sections include estimated contributions from (γ, p) reactions.

^b The correction "W" is the sum of the high- and low-energy wing corrections to the area under the resonance curves for the oblate case.

values agree within the experimental errors. The measured values, however, include corrections for the (γ, p) cross sections which were obtained by evaporative-model calculations for Cu⁶³, and from the work of Lin Kova *et al.*²⁰ for Cu⁶⁵.

The Lorentz curves, fitted on the assumption that the nuclei have the shapes of oblate spheroids, are characteristic of nuclei having negative quadrupole moments. Those fitted to prolate spheroids are characteristic of nuclei with positive quadrupole moments. The value obtained for the positive and negative quadrupole moments deduced from the two types of fits of the Lorentz curves are given in Table III. The negative values, -1.4 ± 0.4 and -1.1 ± 0.4 b for Cu⁶³ and Cu⁶⁵, respectively, may be compared with those deduced from paramagnetic resonance experiments,²¹ i.e., -0.80 and -0.75 b, respectively. The agreement is not as close as would be considered desirable, but it is possible that some nuclear shell characteristics in the giant resonance may affect these quantities.

From the ratio of $\sigma(\gamma, 2n)$ to the total cross section²² the level density parameters "a" were deduced for Cu⁶³ and Cu⁶⁵ after making corrections for the amount of direct interaction in the case of Cu⁶³. The values of "a" obtained for Cu⁶³ and Cu⁶⁵ were 4 ± 1 and 9 ± 3 (MeV)⁻¹, respectively. These may be compared with 12.06 and 10.31 (MeV)⁻¹, respectively, given by Erba *et al.*,²³ for an excitation energy of 14 MeV, or 6.9 (MeV)⁻¹ for natural Cu given by Thompson²⁴ for an excitation energy of 5.0 MeV.

²¹ D. Strominger, J. M. Hollander, and G. T. Seaborg, *Rev. Mod. Phys.* **30**, No. 2 (1958).

²² J. M. Blatt and V. F. Weisskopf, *Theoretical Nuclear Physics* (John Wiley & Sons, Inc., New York, 1952).

²³ E. Erba, U. Facchini, and E. Saetta Menichella, *Nuovo Cimento* **22**, 1237 (1961).

²⁴ D. B. Thompson, *Phys. Rev.* **129**, 1649 (1963).

SUMMARY AND CONCLUSIONS

Copper is in a transition region of nuclear mass. It is a medium-weight nucleus and not highly deformed. Proton emission is inhibited, but not negligible. Consequently, theories of deformation, sum rules, or evaporation are not simply applied. As previously indicated, the cross-section curves for Cu⁶³ and Cu⁶⁵ could be fitted with Lorentz functions for either prolate or oblate spheroids. If an oblate form is assumed, the intrinsic quadrupole moments obtained are in rough agreement with those obtained by other methods. The integrated cross sections, when corrected for (γ, p) contributions and high-energy wings under the Lorentz curves, are in agreement with those expected from saturation of the dipole sum rule without correction for exchange forces. Also, the values obtained for σ_{-2} are in agreement with those deduced from theory. The estimate of 8% for the amount of direct interaction occurring for the (γ, n) reactions in Cu⁶³ excludes possible contribution to direct interactions which occur in the (γ, p) reactions. It is therefore a very rough estimate and is probably too low.

ACKNOWLEDGMENTS

The authors wish to express their thanks to Dr. F. Buskirk of the Naval Postgraduate School for the statistical-model calculations on Cu⁶³. They also wish to acknowledge the cooperation of the accelerator operators and other supporting personnel, and the support for the program given by the Lawrence Radiation Laboratory.